Exciton polaritons in two-dimensional photonic crystals

D. Bajoni,[1,][*] D. Gerace,[2] M. Galli,[2] J. Bloch,[3] R. Braive,[3] I. Sagnes,[3] A. Miard,[3] A. Lemaître,[3] M. Patrini,[2] and L. C. Andreani[2]

[1]*Dipartimento di Elettronica, Università degli Studi di Pavia and CNISM, via Ferrata 1, 27100 Pavia, Italy*
[2]*Dipartimento di Fisica "A. Volta," Università degli Studi di Pavia and CNISM, via Bassi 6, 27100 Pavia, Italy*
[3]*Laboratoire de Photonique et de Nanostructures, CNRS, Route de Nozay, 91460 Marcoussis, France*
(Received 16 July 2009; revised manuscript received 15 October 2009; published 16 November 2009)

Experimental evidence of strong coupling between excitons confined in a quantum well and the photonic modes of a two-dimensional dielectric lattice is reported. Both resonant scattering and photoluminescence spectra at low temperature show the anticrossing of the polariton branches, fingerprint of strong coupling regime. The experiments show that the polariton dispersion can be tailored by properly varying the photonic crystal lattice parameter, which enlarges the possibility of engineering polariton dispersion.

The strong coupling regime between light and matter is characterized by a reversible and coherent exchange of energy between a single material oscillator and a single mode of the electromagnetic field. A particular case is when excitons confined in a semiconductor quantum well (QW) are spectrally and spatially resonant with the mode of a vertical semiconductor microcavity, e.g., in structures similar to the vertical cavity surface emitting laser.[1] If the coherent light-matter coupling overcomes excitonic and photonic dissipation rates, the strong coupling regime can be achieved in these structures.[2,3] As a result, exciton-photon hybrid quasiparticles named *microcavity polaritons* are formed.

Microcavity polaritons have bosonic statistics, fast interaction with the electromagnetic field, and strong optical nonlinearities related to their excitonic parts. These properties have been exploited to obtain a wealth of nonclassical phenomena in the solid state: coherent and macroscopically occupied matter-wave states,[4,5] optical spin Hall effect,[6] and superfluidity[7] among others. Their strong optical nonlinearities have been used to demonstrate low-power parametric oscillations of matter waves:[8–11] considerable interest has been devoted to polariton parametric scattering with the goal of realizing a semiconductor-based, monolithic, and micronsized source of entangled photon pairs. However, quantum correlation experiments are usually hindered by the great intensity difference between signal and idler beams, which is intrinsic to the dispersion of polariton branches in planar microcavities:[12] possible solutions have been sought by modifying the microcavity geometry.[10,13]

Photonic crystals can be used to tune the photonic mode dispersion by suitably modifying the sample design,[14] as it can be measured via reflectance or transmittance from the sample surface.[15–17] Thus, photonic crystals in the strong coupling regime give the unique possibility to engineer the dispersion of polariton branches. New ways to achieve phase matching for parametric scattering, e.g., to obtain signal and idler beams of comparable intensity, can thus be envisioned, opening the possibility of measuring quantum correlations between signal and idler polaritons. Early experimental evidence of polaritons in photonic crystals has been reported by using perovskites sputtered on gratings.[18–21] Although theoretically proposed,[22] polaritons in photonic crystals have never been reported in semiconductors, where highly efficient parametric scattering is quite well characterized.[11] The

main problem is that, in many semiconductor systems and in particular in GaAs-based samples, patterning the QW results in a severe reduction of the exciton lifetime by nonradiative recombination at hole sidewalls[23] and consequently in the loss of strong coupling.[24]

Here we report the experimental evidence of strong coupling between excitons confined in a semiconductor QW and the photonic modes of a two-dimensional photonic crystal. To avoid issues related to nonradiative recombination, we adopt an original design: the photonic lattice is spatially separated from the QWs so that polaritons only experience the periodic potential through their photonic part while leaving the QW intact.

The sample, schematically shown in Fig. 1(a), was grown by molecular beam epitaxy on a GaAs substrate. A 140-nm-thick $Al_{0.8}Ga_{0.2}As$ cladding was first deposited, followed by a 148-nm-thick GaAs core with three 8-nm-thick $In_{0.05}Ga_{0.95}As$ QWs at its center, a second 140-nm-thick $Al_{0.8}Ga_{0.2}As$ cladding, and finally a 100 nm GaAs top layer. The top layer was patterned by inductively coupled plasma etching[25] with a square lattice of circular air holes [see Fig. 1(b)]: areas with different lattice parameters $a=245$, 250, 255, and 260 nm were defined (the patterned areas have 50 μm side). The nominal etch depth is 120 nm. The periodic corrugation yields a dispersion folding on the *guided* modes of the slab waveguide within the first Brillouin zone [Fig. 1(d), upper panel], making them *radiative* around normal incidence (Γ point). Such folding depends on the lattice parameter a: for different lattice parameters, the resonance condition between the QW exciton and the photonic modes changes within the dispersion diagram. This is the essence of the polariton dispersion engineering discussed in the following, and it is shown in the calculated mode dispersion in Fig. 1(d).

The sample was kept at low temperature in a He-cooled cold finger cryostat. The experimental setup is outlined in Fig. 1(c). To probe the elementary excitations of the system two different techniques were used: photoluminescence (PL) and resonant scattering (RS) of white light. This latter approach relies on sending a linearly polarized white light beam along the y axis [by the polarizer $\vec{P}$ in Fig. 1(c)] and analyzing the reflected light in crossed polarization through a second polarizer along $x (\vec{A})$. The photonic modes of the
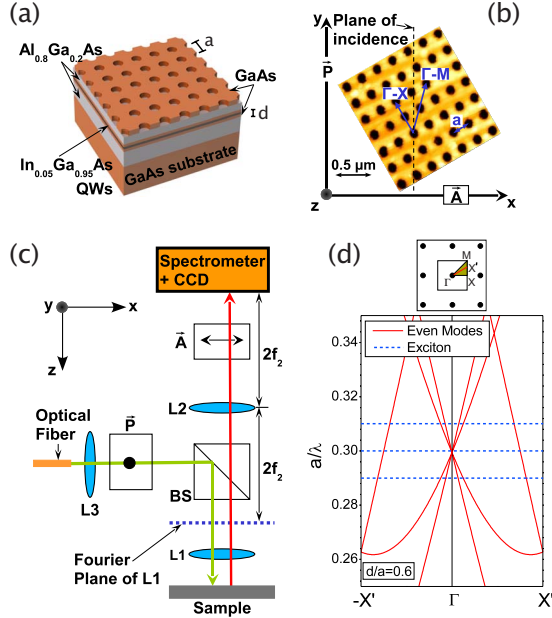
FIG. 1. (Color online) (a) Schematic sample structure. Relevant parameters are the waveguide core thickness, d, and the lattice constant, a. (b) Atomic force microscope image of the surface of a sample with $a=250$ nm. The main lattice directions, as well as the plane of incidence and the orientation of the polarizers, are shown. (c) Experimental setup: the green line is the incoming beam (laser or white light) and the red line is the output beam (PL or reflected light), while $\vec{A}$ and $\vec{P}$ are two linear polarizers, L_1, L_2, and L_3 are lenses, f_2 is the focal length of L_2, and BS is a beam splitter. (d) Schematic Brillouin zone and guided mode dispersion in the experimental plane of incidence; notice that the energy scale is in adimensional units. The modes are calculated for a symmetric planar GaAs waveguide with between AlGaAs claddings, with dielectric constants $\varepsilon_{core}=12.97$ and $\varepsilon_{clad}=9.5$, respectively. The exciton resonance for three different lattice parameters is represented with dashed lines.

sample have a symmetry that can be even (i.e., having the electric field mainly polarized in the QW plane, TE-like) or odd (i.e., with the electric field mainly polarized perpendicular to the QW plane, TM-like). A crucial point in the present experiment is that the plane of incidence is tilted by $\phi=30°$ with respect to the ΓX lattice direction [Figs. 1(b) and 1(c)] and is not a mirror plane of the structure. While most of the reflected light keeps the polarization specified by the polarizer $\vec{P}$, when the incoming beam is resonant with a photonic or polaritonic mode a small amount of light is coupled to the opposite polarization, i.e., parallel to $\vec{A}$.[26] The RS signal, essentially due to polarization rotation in reflection, is a measure of the extinction of light due to its coupling with the sample and can be used to probe the dispersion of the modes in a wide spectral range. PL spectra are obtained on the same setup employing a laser pump at 1550 meV. Both the laser pump and the white light beam are focused on a 20 μm diameter spot on the sample surface by a microscope objective [L_1 in Fig. 1(a)], which is also used to collect the emitted or reflected light. The plane of incidence is determined by the entrance slit of the spectrophotometer (parallel to y in the frame of Fig. 1) and resolution in the angle of incidence (ϑ)
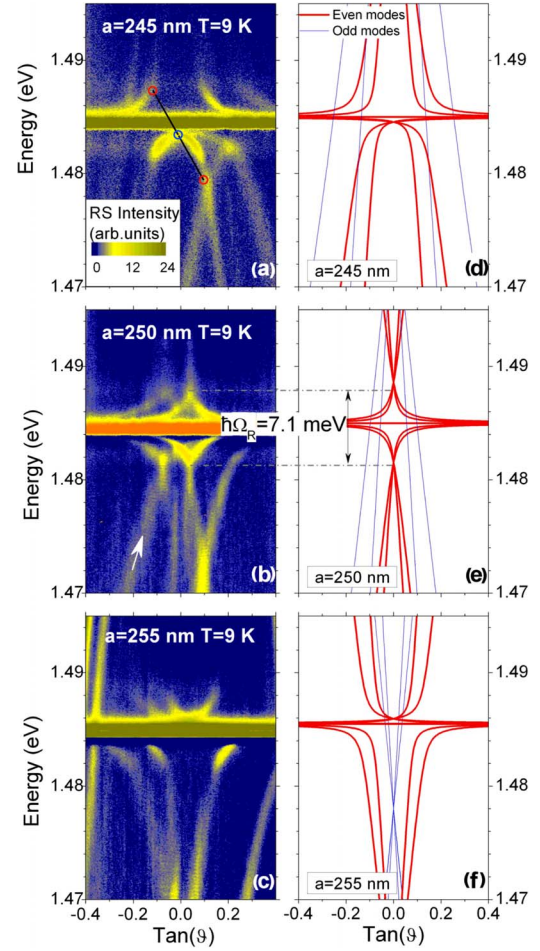
FIG. 2. (Color online) Experimental RS spectra for samples with lattice constants (a) $a=245$, (b) 250, and (c) 255 nm. (d)–(f) Corresponding calculated dispersion curves for even (red) and odd (blue) modes. A possible parametric scheme for entangled photon generation is indicated in (a). The central dot indicates the energy and angle for the pump beam, while the low and high energy dots indicate the signal and idler beams, respectively. The equiseparation in energy and wave vectors of the three states grants the phase matching condition for four-wave mixing.

is obtained by directly imaging the Fourier plane of L_1 onto the slit.

Polariton states, i.e., mixed radiation-matter quasiparticles, are expected to occur when the dimensionality of photon states is equal to (or, possibly, smaller than) that of the exciton.[27] Given the energies E_X and E_{Ph} of the uncoupled exciton and photonic modes and the respective dissipation rates γ_X and γ_{Ph}, the energies of the polariton eigenstates are simply described by[3]

$$E_{LP/UP} = \frac{1}{2}(E_X + i\gamma_X + E_{Ph} + i\gamma_{Ph})$$
$$\mp \frac{1}{2}\sqrt{(\hbar\Omega_R)^2 + (E_X + i\gamma_X - E_{Ph} - i\gamma_{Ph})^2}, \quad (1)$$

where $\hbar\Omega_R/2$ is the coupling constant between excitons and photons (half of the vacuum Rabi splitting). Equation (1) implies that polaritons anticross in reciprocal space, where the uncoupled modes would cross instead: the observation of
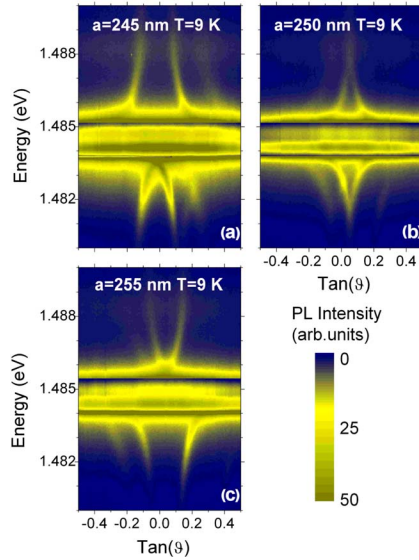
FIG. 3. (Color online) Experimental PL spectra for samples with lattice constants (a) $a=245$, (b) 250, and (c) 255 nm. The intensity has been divided by a factor of 5 in a window of ~1.3 meV around the exciton resonance.

FIG. 4. (Color online) Experimental PL spectra for a sample with $a=260$ nm at temperatures (a) $T=8$, (b) 70, and (c) 250 K, respectively. In panels (a) and (b), the intensity in a window of ~1.3 meV around the exciton resonance has been divided by a factor of 5. (d) Energies of the exciton (red tilted square), mode 1 [black circles, black circle in panel (b)], mode 2 [black triangles, black circle in panel (b)], and mode 3 [green tilted square, green circle in panel (c)] as a function of temperature. The green dashed line is the uncoupled photonic mode at $\vartheta=10°$ (i.e., $\tan\vartheta \sim 0.18$).

such anticrossing is a clear signature of the strong coupling regime.

Low temperature RS measurements as a function of the incidence angle, ϑ, are shown in Figs. 2(a)–2(c) for samples with $a=245$, 250, and 255 nm, respectively. All spectra display an anticrossing between the dispersive modes and the exciton line at 1.485 eV, proving the occurrence of a strong coupling regime. Both the upper and lower polariton branches are clearly visible on either side of the exciton and the polariton linewidth remains well below 1 meV in all spectra; the measured Rabi splitting is $\simeq 7$ meV, comparable to what has been reported for planar microcavities. Notice that, without coupling with the exciton, the modal dispersion would be linear, as discussed below. Figure 2 highlights the original shape of polariton dispersions in such photonic crystals: for instance, the diamondlike shape of the modes in Fig. 2(b) is completely different from the S-shaped dispersion of microcavity polaritons.[3,18] Moreover the polariton dispersion dramatically depends on the lattice constant: changing a by only 2% (5 nm) substantially reshapes the branches. In Fig. 2(a) we indicate a possible scheme for implementing a four-wave mixing experiment with our device, in which the signal and idler beams have about the same photonic fraction (to within 10%), an important requirement for the generation of entangled pairs.

We model the system under investigation by calculating the photonic modes for the planar waveguide in the two-dimensional lattice as in Fig. 1(d) and coupling them to the QW exciton envelope function.[22] The Rabi splitting in the polariton mode dispersion depends on the oscillator strength per unit area.[28] The resulting polariton dispersions are reported in Figs. 2(d)–2(f) for the same lattice parameters as in Figs. 2(a)–2(c). Overall, the details of the polariton modes are complicated by the tilted plane of incidence (30°) with respect to the ΓX direction, which removes photonic mode

degeneracies. Two photonic branches for each parity can be distinguished at the Γ point ($\vartheta=0°$), but only even modes strongly couple to the excitons. There is a good agreement between theory and experiment: the calculated Rabi splitting for these structures is $\hbar\Omega_R \simeq 7.1$ meV and compares very well with the experimentally determined value of ~7 meV, as it can be easily seen by directly comparing Figs. 2(b) and 2(e). Notice the presence of additional polariton branches in the measurements, which are not reproduced by the theory [an instance is highlighted by a white arrow in Fig. 2(b)]. These additional modes disappear when the plane of incidence corresponds to a high symmetry direction of the lattice (ΓM or ΓX) and may be related to effects on the border of the patterned areas: further theoretical and experimental investigation is underway to investigate the origin of the additional features.

Measured PL spectra are shown in Figs. 3(a)–3(c). At such low temperatures, only polariton states lying a few meV from the exciton are enough populated to efficiently contribute to the PL signal, and the energy scale is consequently expanded in the figure. Polariton dispersion lines in emission are exactly equivalent to those reported in RS, confirming the occurrence of strong coupling in these samples. The exciton line at 1.485 eV is much more intense than the polariton lines. This is mainly due to two reasons: first, in the

present experiment we collect the PL signal on a much wider region than the excitation spot, so that we measure also the signal coming from diffused excitons outside the patterned region; second, only exciton states with symmetry close to the photonic mode are strongly coupled, while the majority of states remain in weak coupling with the electromagnetic field.[22] A rough estimation of the fraction of excited excitons which are involved in the strong coupling regime can be obtained by comparing the photoluminescence signal intensity of the polariton modes (weighted with their photonic fraction) and the signal from the exciton, yielding a fraction of about 1% of the detected energy coming from polaritons.

To evidence the difference between strong and weak couplings in our samples, PL measurements with increasing temperature (T) are plotted in Figs. 4(a)–4(c) for a sample with $a=260$ nm. At $T=70$ K the sample is still in strong coupling and shows the same anticrossing at $T=8$ K [Figs. 4(a) and 4(b)]. Above 80 K the Rabi splitting is progressively reduced and at $T=250$ K [Fig. 4(c)] strong coupling is lost and the photonic modes cross the exciton resonance. As an illustration, Fig. 4(d) shows the energy variation with temperature of the exciton and of three modes chosen around the exciton at $\vartheta=10°$ [modes 1 and 2; see black circles in Figs. 4(a) and 4(b)] and at low energy at $\vartheta=0°$ [mode 3; see black circle in Fig. 4(c)] extracted from the spectra. Since the exciton redshift is stronger than that of the photonic modes, increasing temperature changes the detuning between exciton and modes. The exciton and mode 3 cross above 200 K, which evidences that they are in weak coupling. On the other hand, modes 1 and 2 anticross at 45 K and are thus in strong coupling. Their energies can be fitted by using Eq. (1), in

which the uncoupled photonic mode, E_{Ph}, is assumed to have the same dependence on the temperature as mode 3. This loss of strong coupling at high temperature can be understood considering the exciton dephasing rate γ_X in Eq. (1): increasing temperature means increasing γ_X until the term under square root becomes negative, i.e., excitons dephase in a time $1/\gamma_X$ before a single Rabi oscillation can be completed.

In conclusion, we have shown the strong coupling regime of quantum-well excitons in two-dimensional photonic crystals through both resonant scattering and photoluminescence experiments at low temperature. The present results will open directions for polariton research: the possibility of engineering phase matching is a considerable step toward achieving a compact and integrable solid-state source of entangled photon pairs. Further applications can be envisioned for polaritons in large band gap materials. Although the strong coupling regime has been already reported at room temperature in high band gap materials,[29] fabrication of high quality microcavities for these materials is often impractical due to the large number of required layers. Using planar photonic crystals, and in particular the present design that leaves the active region intact, will turn to be effective for obtaining strong coupling with high quality optical modes at room temperature.

*daniele.bajoni@unipv.it
[1] K. Iga, IEEE J. Sel. Top. Quantum Electron. **6**, 1201 (2000).
[2] C. Weisbuch, M. Nishioka, A. Ishikawa, and Y. Arakawa, Phys. Rev. Lett. **69**, 3314 (1992).
[3] M. S. Skolnick *et al.*, Semicond. Sci. Technol. **13**, 645 (1998).
[4] J. Kasprzak *et al.*, Nature (London) **443**, 409 (2006).
[5] R. Balili *et al.*, Science **316**, 1007 (2007).
[6] C. Leyder *et al.*, Nat. Phys. **3**, 628 (2007).
[7] A. Amo *et al.*, Nature (London) **457**, 291 (2009); A. Amo *et al.*, Nat. Phys. **5**, 805 (2009).
[8] P. G. Savvidis, J. J. Baumberg, R. M. Stevenson, M. S. Skolnick, D. M. Whittaker, and J. S. Roberts, Phys. Rev. Lett. **84**, 1547 (2000).
[9] R. M. Stevenson, V. N. Astratov, M. S. Skolnick, D. M. Whittaker, M. Emam-Ismail, A. I. Tartakovskii, P. G. Savvidis, J. J. Baumberg, and J. S. Roberts, Phys. Rev. Lett. **85**, 3680 (2000).
[10] C. Diederichs *et al.*, Nature (London) **440**, 904 (2006).
[11] M. Saba *et al.*, Nature (London) **414**, 731 (2001).
[12] J. Ph. Karr, A. Baas, and E. Giacobino, Phys. Rev. A **69**, 063807 (2004).
[13] D. Bajoni *et al.*, Appl. Phys. Lett. **90**, 051107 (2007).
[14] J. D. Joannopoulos, S. G. Johnson, J. N. Winn, and R. D. Meade, *Photonic Crystals: Molding the Flow of Light* (Princeton University Press, Princeton, 2008).
[15] D. M. Whittaker and I. S. Culshaw, Phys. Rev. B **60**, 2610 (1999).
[16] V. N. Astratov, D. M. Whittaker, I. S. Culshaw, R. M. Stevenson,

M. S. Skolnick, T. F. Krauss, and R. M. De La Rue, Phys. Rev. B **60**, R16255 (1999).
[17] A. R. Cowan and J. F. Young, Phys. Rev. B **65**, 085106 (2002).
[18] T. Fujita, Y. Sato, T. Kuitani, and T. Ishihara, Phys. Rev. B **57**, 12428 (1998).
[19] R. Shimada *et al.*, IEEE J. Quantum Electron. **38**, 872 (2002).
[20] J. Ishi-Hayase and T. Ishihara, Semicond. Sci. Technol. **18**, S411 (2003).
[21] M. Shimizu and T. Ishihara, Appl. Phys. Lett. **80**, 2836 (2002).
[22] D. Gerace and L. C. Andreani, Phys. Rev. B **75**, 235325 (2007).
[23] D. Englund *et al.*, Appl. Phys. Lett. **91**, 071124 (2007).
[24] T. Stroucken *et al.*, J. Opt. Soc. Am. B **19**, 2292 (2002).
[25] R. Braive *et al.*, Opt. Lett. **34**, 554 (2009).
[26] M. McCutcheon *et al.*, Appl. Phys. Lett. **87**, 221110 (2005); M. Galli *et al.*, *ibid.* **94**, 071101 (2009).
[27] L. C. Andreani, in *Electron and Photon Confinement in Semiconductor Nanostructures*, edited by B. Deveaud, A. Quattropani, and P. Schwendimann (IOS Press, Amsterdam, 2003), p. 105.
[28] We take $f/S=4.5\times10^{12}$ cm^{-2} [R. C. Iotti and L. C. Andreani, Phys. Rev. B **56**, 3922 (1997)] and multiply it by $\sqrt{3}$ to simulate the fabricated structure with three QWs in the GaAs core. No other adjustable parameter was used in the theoretical analysis.
[29] F. Semond *et al.*, Appl. Phys. Lett. **87**, 021102 (2005); R. Butté, G. Christmann, E. Feltin, J.-F. Carlin, M. Mosca, M. Ilegems, and N. Grandjean, Phys. Rev. B **73**, 033315 (2006); R. Shimada *et al.*, Appl. Phys. Lett. **92**, 011127 (2008).